

# High Superoxide Dismutase Activity of a Novel, Intramolecularly Imidazolato-Bridged Asymmetric Dicopper(II) Species. Design, Synthesis, Structure, and Magnetism of Copper(II) Complexes with a Mixed Pyrazole–Imidazole Donor Set

Giovanni Tabbì,<sup>†,‡</sup> Willem L. Driessen,<sup>†</sup> Jan Reedijk,<sup>\*,†</sup> Raffaele P. Bonomo,<sup>§</sup> Nora Veldman,<sup>||</sup> and Anthony L. Spek<sup>||</sup>

Leiden Institute of Chemistry, Gorlaeus Laboratories, Leiden University, P.O. Box 9502, 2300 RA Leiden, The Netherlands, Department of Chemical Sciences, University of Catania, Viale A. Doria 6, 95125 Catania, Italy, and Bijvoet Center for Biomolecular Research, Utrecht University, Padualaan 8, 3584 CH Utrecht, The Netherlands

Received October 18, 1996<sup>®</sup>

A new dinucleating ligand, 1,5-bis(1-pyrazolyl)-3-[bis(2-imidazolyl)methyl] azapentane (Hbpzbiap), containing pyrazoles and imidazoles has been designed and synthesized. The synthesis and characterization of the copper complexes with the ligand Hbpzbiap and its dehydrated form are described. This study is aimed at modeling the active site of copper–zinc superoxide dismutase (SOD). Single crystals of the imidazolato-bridged complex [Cu<sub>2</sub>(bpzbiap)Cl<sub>3</sub>] (**1**) and non-imidazolato-bridged complex [Cu<sub>2</sub>(Hbpzbiap)Cl<sub>4</sub>] (**2**) were obtained and their structures determined by X-ray diffraction. Both structures show two copper centers in two different coordination environments: a distorted square pyramid and a distorted tetrahedron. The Cu–nitrogen bond lengths range from 1.919(4) to 2.039(3) Å and are as expected. The copper–copper distances from 5.566(1) to 6.104(1) Å being only slightly shorter than that found in bovine erythrocyte SOD. Temperature-dependent magnetic susceptibility study of **1** shows antiferromagnetic behavior with  $-2J = 96 \text{ cm}^{-1}$ . From pH-dependent electron paramagnetic resonance and electronic spectra, [Cu<sub>2</sub>(bpzbiap)Cl<sub>3</sub>] has been demonstrated to be stable over a quite wide pH range including the physiological pH values. A low concentration of this complex (**1**) catalyzes the dismutation of superoxide at biological pH. Voltammetric studies indicate a quasi-reversible redox behavior in aqueous solution at pH 7. These results clearly indicate that complex **1** is a good model for superoxide dismutase.

## Introduction

The biological activity of metalloproteins is almost always associated with a particular coordination environment of the metal active site. Crystallographic studies of copper–zinc superoxide dismutase (SOD)<sup>1</sup> clearly showed the presence of an imidazolato-bridged dinuclear center containing copper(II) and zinc(II) ions as active site. The coordination geometry is distorted square-pyramidal for copper(II) and distorted tetrahedral for zinc(II). The presence of a dinuclear center in superoxide dismutase was also confirmed by preparing the dinuclear metal(II) derivatives of the native enzyme.<sup>2</sup>

The synthesis of low-molecular weight copper(II) complexes mimicking the SOD activity has been challenging for bioinorganic chemists and for many years efforts have been made to obtain compounds with high catalytic activity.<sup>3–17</sup>

In designing such a dinuclear complex several approaches have been used. Good models have been obtained using metal macrocycle complexes and adding imidazole to the preformed complex.<sup>3–7, 9,11–13,15–17</sup> This approach leads to chemical models having a good stability over a broad pH range. Alternatively, open-chain ligands bearing an imidazole moiety have been used, but in this case the chelate effect is used to enhance the stability in solution.<sup>8,10,14</sup> Many SOD-like models are scarcely water soluble or are not stable in the presence of water. Thus, it could be particularly useful to include the imidazole moiety in a chelating ligand that stabilizes the complex species in a wide pH range.

Important requirements for SOD-like activity are a medium strength donor power and the flexibility of the ligands, in order to facilitate the reduction and the accommodation of copper(I), which is known to prefer tetrahedral or linear environments.<sup>18–20</sup> Interestingly, several copper(II) complexes having imidazole

<sup>†</sup> Leiden University.

<sup>‡</sup> Research Fellow on leave from: Department of Chemical Sciences, University of Catania, Viale A. Doria 6, 95125 Catania, Italy.

<sup>§</sup> University of Catania.

<sup>||</sup> Utrecht University.

<sup>®</sup> Abstract published in *Advance ACS Abstracts*, February 15, 1997.

- (1) Tainer, J. A.; Getzoff, E. D.; Richardson, J. S.; Richardson, D. C. *Nature* **1983**, *306*, 284.
- (2) Fee, J. A.; Briggs, R. G. *Biochim. Biophys. Acta* **1975**, *400*, 439.
- (3) Strotkamp, K. G.; Lippard, S. J. *Acc. Chem. Res.* **1982**, *15*, 318.
- (4) Gartner, A.; Weser, U. *Top. Curr. Chem.* **1986**, *132*, 1.
- (5) Murphy, B. P. *Coord. Chem. Rev.* **1993**, *124*, 63.
- (6) Pierre, J.-L.; Chautemps, P.; Refaif, S.; Beguin, C.; El Marzouki, A.; Serratrice, G.; Saint-Aman, E.; Rey, P. *J. Am. Chem. Soc.* **1995**, *117*, 1965.
- (7) Weser, U.; Schubotz, L. M.; Lengfelder, E. *J. Mol. Catal.* **1981**, *13*, 249.
- (8) O'Young, C.-L.; Dewan, J. C.; Lilienthal, H. R.; Lippard, S. J. *J. Am. Chem. Soc.* **1978**, *100*, 7291.

- (9) Coughlin, P. K.; Martin, A. E.; Dewan, J. C.; Watanabe, E.; Bulkowski, J. E.; Lehn, J.-L.; Lippard, S. J. *Inorg. Chem.* **1984**, *23*, 1004.
- (10) Coughlin, P. K.; Lippard, S. J. *Inorg. Chem.* **1984**, *23*, 1446.
- (11) Drew, M. G. B.; Cairns, C.; Lavery, A.; Nelson, S. M. *J. Chem. Soc., Chem. Commun.* **1980**, 1122.
- (12) Drew, M. G. B.; McCann, M.; Nelson, S. M. *J. Chem. Soc., Dalton Trans.* **1981**, 1868.
- (13) Drew, M. G. B.; Nelson, S. M.; Reedijk, J. *Inorg. Chim. Acta* **1982**, *64*, L189.
- (14) Sato, M.; Ikeda, M.; Nakaya, J. *Inorg. Chim. Acta* **1984**, *93*, L61.
- (15) Cabral, J.; Cabral, M. F.; McCann, M.; Nelson, S. M. *Inorg. Chim. Acta* **1984**, *86*, L15.
- (16) Salata, C. A.; Youinou, M. T.; Burrows, C. J. *J. Am. Chem. Soc.* **1989**, *111*, 9278.
- (17) Salata, C. A.; Youinou, M. T.; Burrows, C. J. *Inorg. Chem.* **1991**, *30*, 3454.
- (18) Bonomo, R. P.; Conte, E.; Marchelli, R.; Santoro, A. M.; Tabbì, G. *J. Inorg. Biochem.* **1994**, *53*, 127.

moieties coordinated in a distorted tetrahedral geometry show acceptable SOD-like activity.<sup>21–23</sup>

Since, in the native SOD, the metal sites are coordinated only by imidazole nitrogens, coming from histidine residues,<sup>1</sup> a new ligand containing imidazoles and pyrazoles was designed and its dinuclear copper(II) complexes synthesized and characterized.

In this paper, we report the synthesis of such a novel ligand, 1,5-bis(1-pyrazolyl)-3-[bis(2-imidazolyl)methyl]azapentane (Hbpbziap) and two dicopper(II) complexes, their X-ray crystal structure determination, the result of magnetic susceptibility, EPR, cyclic voltammetry, electronic spectroscopic investigations, and SOD-like activity. Both complexes only differ in the presence/absence of an imidazolato-bridge.

## Experimental Section

**Materials and Methods.** Commercial reagents were used as obtained without further purification. Elemental analyses were performed by the Microanalytical Laboratory of University College, Dublin, Ireland.

**Syntheses. 1,5-Bis(1-pyrazolyl)-3-[bis(2-imidazolyl)methyl]azapentane (Hbpbziap).** A 3.6 g (15.7 mmol) sample of bis[imidazol-2-yl]nitromethane (binm)<sup>24</sup> was added to 35 mL of absolute ethanol containing 3.6 g (17.5 mmol) of bis[2-(1-pyrazolyl)ethyl]amine (bpea).<sup>25</sup> To the resulting mixture was added 3 mL of aqueous NaOH (0.68 g, 17 mmol) was added under stirring and the suspension was stirred at 40 °C for 4 days, cooled, and filtered. The solvent was completely evaporated under reduced pressure. The starting material, binm, was precipitated by dissolving the oily residue in 2 mL of methanol and adding 50 mL of diethyl ether under stirring. The filtered sample was purified on column (Kieselgel 60 Merck) eluting with CH<sub>2</sub>Cl<sub>2</sub>/MeOH 80/20. The fractions containing the product (*R<sub>f</sub>* 0.8) were gathered and the solvent evaporated. After evaporation 1.74 g of yellow oil was obtained (yield: 30%).

<sup>1</sup>H NMR (CD<sub>3</sub>OD): δ 2.90 (4H, t, *J* = 6 Hz, CH<sub>2</sub>N), 4.06 (4H, t, *J* = 6 Hz, CH<sub>2</sub>Pz), 5.29 (s, 1H, CH), 5.78 (s, 2H, PzH), 6.26 (2H, t, *J* = 2 Hz, C<sub>4</sub>PzH), 7.03 (s, 4H, ImH), 7.42 (2H, d, *J* = 2 Hz, C<sub>3</sub>PzH), 7.47 (2H, d, *J* = 2 Hz, C<sub>5</sub>PzH).

**[Cu<sub>2</sub>(bpbziap)Cl<sub>3</sub>] (1).** An ethanolic solution of CuCl<sub>2</sub>·2H<sub>2</sub>O (47 mg, 0.278 mmol, 15 mL) was added under stirring at room temperature to a solution of Hbpbziap (49 mg, 0.139 mmol) in ethanol (20 mL, 96%). After 2 min, 1.4 mL of 0.1 M NaOH was added under stirring. After 1 week, green crystals began to appear from the green solution. After 3 weeks, the crystals were collected by filtration and dried in air (yield 27 mg, 33.3%). Anal. Calcd for C<sub>17</sub>H<sub>20</sub>Cl<sub>3</sub>Cu<sub>2</sub>N<sub>9</sub>: C, 34.97; H, 3.45; Cl, 18.22; Cu, 21.77; N, 21.59. Found: C, 35.05; H, 3.40; Cl, 18.02; Cu, 21.55; N, 21.68.

**[Cu<sub>2</sub>(Hbpbziap)Cl<sub>4</sub>] (2).** An ethanolic solution of CuCl<sub>2</sub>·2H<sub>2</sub>O (24 mg, 0.139 mmol, 15 mL) and ZnCl<sub>2</sub> (19 mg, 0.139 mmol) was added to a solution of Hbpbziap (49 mg, 0.139 mmol) in ethanol (20 mL, 96%) under stirring at room temperature. After 2 days, green crystals began to appear from the green solution. After 4 weeks, the crystals were collected by filtration and dried in air. Microscope analysis showed that two kinds of crystals were present: the first having the same shape and color of **1** and the second which were more regular and light green. Only few crystals of the latter kind were obtained and used for X-ray diffraction and for EPR measurements.

**X-ray Structure Determination of 1 and 2.** X-ray data were collected at 150 K on an Enraf-Nonius CAD4T on a rotating anode. Data were corrected for absorption using DIFABS as implemented in

**Table 1.** Crystallographic Data for [Cu<sub>2</sub>(bpbziap)Cl<sub>3</sub>] (**1**) and [Cu<sub>2</sub>(bpbziap)Cl<sub>4</sub>] (**2**)

	<b>1</b>	<b>2</b>
formula	C <sub>17</sub> H <sub>20</sub> Cl <sub>3</sub> Cu <sub>2</sub> N <sub>9</sub>	C <sub>17</sub> H <sub>21</sub> Cl <sub>4</sub> Cu <sub>2</sub> N <sub>9</sub>
fw	583.86	620.32
color	greenish	greenish
space group	monoclinic <i>P2<sub>1</sub>/c</i>	orthorhombic <i>Pca2<sub>1</sub></i>
<i>a</i> (Å)	8.4202(6)	16.4548(8)
<i>b</i> (Å)	19.2442(15)	11.7331(8)
<i>c</i> (Å)	15.5336(13)	12.3265(8)
β (deg)	122.576(5)	
<i>V</i> (Å <sup>3</sup> )	2121.1(3)	2379.8(3)
λ Mo(Kα) (Å)	0.71073	0.71073
<i>Z</i>	4	4
ρ (g·cm <sup>-3</sup> )	1.8282(3)	1.7312(2)
μ(Mo Kα) (cm <sup>-1</sup> )	24.2	22.7
<i>R</i> [ <i>F</i> > 4σ( <i>F</i> )] <sup>a</sup>	0.0402	0.0471
wR <sub>2</sub> <sup>b</sup>	0.0930	0.0911

$$^a R = \sum(F_o - F_c) / \sum wF_o. \quad ^b wR_2 = [\sum w(F_o^2 - F_c^2)^2 / \sum w(F_o^2)^2]^{1/2}, w = 1/(\sigma^2(F_o^2)).$$

**Table 2.** Selected Bond Lengths (Å) and Bond Angles (deg) for [Cu<sub>2</sub>(bpbziap)Cl<sub>3</sub>] (**1**)

Cu1–Cl3	2.2378(11)	Cu2–Cl5	2.2920(10)
Cu1–Cl4	2.2413(13)	Cu2–N17	2.280(3)
Cu1–N13	1.985(4)	Cu2–N21	1.919(4)
Cu1–N23	1.942(3)	Cu2–N32	1.951(4)
		Cu2–N42	2.212(4)
N21–C22	1.336(5)	N23–C22	1.338(6)
N21–C25	1.368(6)	N23–C24	1.384(5)
C24–C25	1.353(6)		
Cl3–Cu1–Cl4	94.13(4)	Cl5–Cu2–N32	92.82(9)
Cl3–Cu1–N13	94.96(9)	Cl5–Cu2–N42	98.76(8)
Cl3–Cu1–N23	145.48(9)	N17–Cu2–N21	80.73(12)
Cl4–Cu1–N13	152.09(12)	N17–Cu2–N32	90.47(12)
Cl4–Cu1–N23	96.52(10)	N17–Cu2–N42	88.03(11)
N13–Cu1–N23	90.75(14)	N21–Cu2–N32	164.45(16)
Cl5–Cu2–N17	172.38(8)	N21–Cu2–N42	101.23(15)
Cl5–Cu2–N21	94.49(9)	N32–Cu2–N42	91.17(15)
Cu1–N23–C22	125.3(3)	Cu2–N21–C22	115.9(3)
Cu1–N23–C24	125.8(3)	Cu2–N21–C25	133.8(3)
C22–N21–C25	106.2(4)	N23–C24–C25	109.2(4)
C22–N23–C24	104.5(3)	N21–C25–C24	107.6(4)
N21–C22–N23	112.5(4)		
Cu1–N23–N21	153.49(18)	Cu2–N21–N23	146.33(16)
		Cl3···N11	3.462(4)

PLATON.<sup>26</sup> The structures were solved by automatic Patterson techniques (DIRDIF<sup>27</sup>) and refined by full-matrix least-squares methods on *F*<sup>2</sup> with SHELXL-93.<sup>28</sup> Non-hydrogen atoms were refined with anisotropic displacement parameters. Hydrogen atoms were introduced at calculated positions and refined riding on their carrier atoms with isotropic displacement parameters related to the *U*<sub>eq</sub> of the atoms they are attached to. The structure of **2** was refined in its correct absolute structure [Flack parameter 0.02(2)]. Selected numerical data are given in Table 1. Selected bond lengths and angles are listed in Tables 2 and 3. Full details may be found in the Supporting Information. Several trials for refining structure **2** were carried out assuming **2** to be a copper–zinc complex, but the residual map density indicated that **2** is actually a dicopper complex. This hypothesis was supported by the best fit of the electron density map and agreed with the elemental analyses.

**Magnetic Measurements.** Magnetic data were gathered in the 4–270 K range with a fully automated Manics DSM-8 susceptometer equipped with a TBT continuous-flow cryostat and a Drusch EAF 16

(19) Bonomo, R. P.; De Flora, A.; Rizzarelli, E.; Santoro, A. M.; Tabbì, G.; Tonetti, M. *J. Inorg. Biochem.*, **1995**, *59*, 773.

(20) Bonomo, R. P.; Marchelli, R.; Tabbì, G. *J. Inorg. Biochem.*, **1995**, *60*, 205.

(21) Kubota, S.; Yang, J. T. *Proc. Natl. Acad. Sci. U.S.A.* **1984**, *84*, 3283.

(22) Costanzo, L. L.; De Guidi, G.; Giuffrida, S.; Rizzarelli, E.; Vecchio, G. *J. Inorg. Biochem.* **1993**, *50*, 273.

(23) Condorelli, G.; Costanzo, L. L.; De Guidi, G.; Giuffrida, S.; Rizzarelli, E.; Vecchio, G. *J. Inorg. Biochem.* **1994**, *54*, 257.

(24) Leigh, M. J. T.; Dwain, M. L. *Synthesis* **1977**, 459

(25) Sorrell, T. N.; Jameson, D. L.; O'Connor, C. J. *Inorg. Chem.* **1984**, *23*, 190.

(26) Spek, A. L. *Acta Crystallogr.* **1990**, *A46*, C34

(27) Beurskens, P. T.; Admiraal, G.; Beurskens, G.; Bosman, W. P.; Garcia-Granda, S.; Gould, R. O.; Smits, J. M. M.; Smykalla, C. *The DIRDIF program system*; Technical report of the Crystallography Laboratory, University of Nijmegen: Nijmegen, The Netherlands, 1992.

(28) Sheldrick, G. M., SHELXL-93, Program for Crystal Structure Refinement. University of Göttingen, Germany, 1993.

**Table 3.** Selected Bond Lengths (Å) and Bond Angles (deg) for [Cu<sub>2</sub>(bpzbiap)Cl<sub>4</sub>] (2)

Cu1—Cl2	2.2519(17)	Cu2—Cl5	2.2843(16)
Cu1—Cl3	2.2768(18)	Cu2—N17	2.262(5)
Cu1—Cl4	2.2697(16)	Cu2—N21	1.938(5)
Cu1—N13	2.039(3)	Cu2—N32	1.955(5)
		Cu2—N42	2.157(5)
Cl2—Cu1—Cl3	110.73(6)	Cl5—Cu2—N32	91.93(15)
Cl2—Cu1—Cl4	108.67(6)	Cl5—Cu2—N42	98.21(13)
Cl2—Cu1—N13	110.30(14)	N17—Cu2—N21	80.28(19)
Cl3—Cu1—Cl4	111.16(6)	N17—Cu2—N32	91.80(19)
Cl3—Cu1—N13	103.30(15)	N17—Cu2—N42	94.17(18)
Cl4—Cu1—N13	112.62(14)	N21—Cu2—N32	159.2(2)
Cl5—Cu2—N17	166.16(14)	N21—Cu2—N42	98.9(2)
Cl5—Cu2—N21	91.66(15)	N32—Cu2—N42	100.8(2)
Cl(2)...N(11)	3.292(5)	Cl(3)...N(23)	3.123(5)

NC electromagnet operating at ca. 1.4 T. Data were corrected for magnetization of the sample holder and for the diamagnetic contributions of the constituent atoms by using Pascal constants. Magnetic data were fitted to a dinuclear species using the Bleaney–Bowers relationship.<sup>29</sup>

**Spectroscopic Measurements.** *EPR.* Powder EPR spectra were recorded on a JEOL RE2X electron spin resonance spectrometer operating at X-band frequencies (ca. 9 GHz) and equipped with an EPR 900 continuous-flow cryostat. DPPH was used as external calibrant. The measurements were carried out in the 10–293 K temperature range. EPR spectra on frozen solutions were recorded on a Bruker ER 200 D spectrometer driven by the ESP 3220 data system at 77 K. The magnetic field was also controlled by a gaussmeter, Bruker ER 035 M. The pH of the complex solution was adjusted at the proper value by adding sodium hydroxide or hydrochloric acid, and checking it under stirring by a pH meter, ORION Model. 520 equipped with a combined glass microelectrode. An addition of methanol up to 9% was made in order to increase spectral resolution.

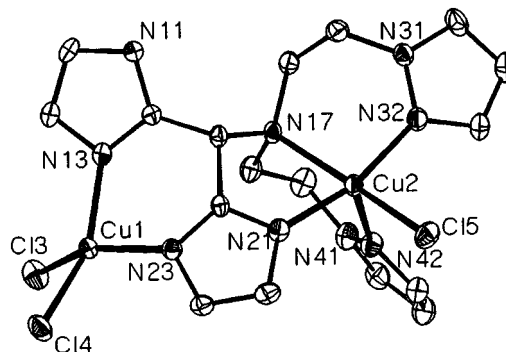
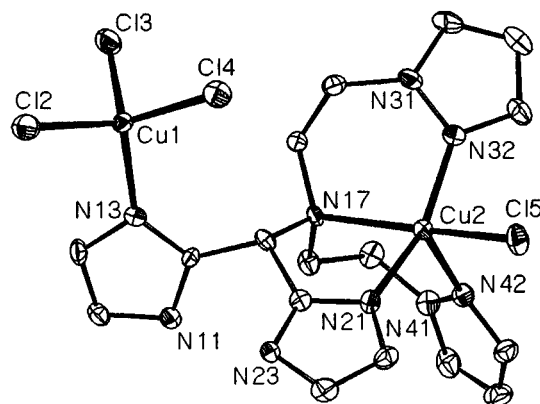
**Vis-Near-IR.** Ligand-field spectra of the solids (300–2000 nm) were recorded on a Perkin-Elmer 330 spectrophotometer equipped with a diffuse reflectance attachment, using MgO as reference.

**UV–Vis.** Spectrophotometric kinetic measurements were carried out on a Hewlett-Packard diode array spectrophotometer, Type 8452, assisted by a Hewlett-Packard computer in thermostated cell equipped with magnetic stirring.

**NMR.** <sup>1</sup>H NMR spectra were recorded on a JEOL JFN-FX 200 FT-NMR spectrometer (working frequency 199.50 MHz) using a 5 mm probe at 25 °C. Chemical shifts were measured in parts per million from internal standard TMS.

**Cyclic Voltammetry.** Cyclic voltammograms were obtained by an Amel model 473 instrument equipped with a 3 mm diameter glassy-carbon disk as working electrode, a saturated calomel electrode (SCE) as reference, and a platinum electrode as auxiliary electrode, respectively. The electrochemical curves were recorded on a AMEL 863 digital X/Y recorder. A solution of complex **1** (0.5 mmol dm<sup>-3</sup>) was prepared by dissolving the appropriate amount of solid complex in twice-distilled water containing 100 mmol dm<sup>-3</sup> KCl as supporting electrolyte, and adjusting the pH at 7.0. The solution was degassed with extrapure nitrogen, which was previously passed on copper wire heated to 450 °C, and a wash bottle. The test solution was thermostated in a bath at a temperature of 25 °C. Cyclic voltammograms with sweep rate ranging from 0.010 to 0.200 V s<sup>-1</sup> were recorded in the region from +0.40 to -0.60 V. Peak currents vs square root of scan rates have been fitted in order to estimate the number of electrons involved in the reduction process.<sup>30</sup>

**Superoxide Dismutase Activity.** Superoxide radical anions were generated by the xanthine–xanthine oxidase system. This method is a slightly modified procedure of Beauchamp and Fridovich.<sup>31</sup> Superoxide radical anions generated by this enzymatic system at pH 7.8 (phosphate buffer, 25 °C) were detected by following spectrophoto-

**Figure 1.** ORTEP representation of **1** with thermal ellipsoids drawn at the 50% probability level.**Figure 2.** ORTEP representation of **2** with thermal ellipsoids drawn at the 50% probability level.

metrically the reduction of nitro blue tetrazolium (NBT) to blue formazan (MF<sup>+</sup>).<sup>32</sup> The appropriate amount of xanthine oxidase (final concentration of 0.07 μM) was added to an aqueous solution of 100 μM NBT, 50 μM xanthine, and phosphate buffer 10 mM (final volume of 2 mL) to cause a variation of absorbance (ΔA<sub>560</sub>/min) of 0.024. This ΔA<sub>560</sub>/min corresponds to a rate of production of superoxide radical of 1.2 mmol dm<sup>-3</sup> min<sup>-1</sup>. The reaction rate in blank samples and in the presence of complex **1** was measured for 300 s only, in order to avoid problems coming from the natural inactivation of the enzymatic system. The system was also tested against a possible inactivation caused by the copper(II) complex itself. The formation of uric acid was kinetically followed at 290 nm to evaluate if the examined complex affects the generation of superoxide anions by directly interacting with the enzymatic system.

## Results

**Preparation and Characterization of Hbpzbiap, [Cu<sub>2</sub>(bpzbiap)Cl<sub>3</sub>] (1), and [Cu<sub>2</sub>(Hbpzbiap)Cl<sub>4</sub>] (2). General Remarks.** The ligand Hbpzbiap has demonstrated a high selectivity in binding copper(II) ions. When the metal to ligand ratio is equal to 2 or higher, compound **1** is readily formed and crystals of it began to appear after few days. If less copper(II) is used, a mixture of compounds **1** and **2** is obtained, even when a stoichiometric amount of zinc is present. This latter trial was made in order to obtain the heterodinuclear compound bearing both copper(II) and zinc(II). Further work to obtain crystals suitable for X-ray diffraction of this compound is in progress.

**Crystal Structure Descriptions.** The ORTEP projections<sup>33</sup> of compounds **1** and **2** are showed in Figures 1 and 2, respectively. Compound **1** crystallizes in the monoclinic space group *P*2<sub>1</sub>/*c*, while **2** crystallizes in the orthorhombic space

(29) Bleaney, B.; Bowers, K. D. *Proc. R. Soc. London, A* **1952**, *214*, 451.

(30) Bond, A. M. *Modern Polarographic Methods in Analytical Chemistry*; Marcel Dekker Inc.: New York, 1980.

(31) Beauchamp, C.; Fridovich, I. *Anal. Biochem.* **1971**, *44*, 276.

(32) Bielski, H. J.; Shiuie, G. G.; Bajuk, S. *J. Phys. Chem.* **1980**, *84*, 830.

(33) Spek, A. L., WINPL96, Interactive Molecular Graphics and Calculations Program for Windows. University of Utrecht, Utrecht, 1996.

group  $Pca2_1$ . Both coordination compounds are characterized by the presence of two copper(II) sites with different environments. In complex **1**, the Cu1 atom is coordinated by the imidazolate nitrogen N23, the imidazole nitrogen N13 and two chloride ions Cl3 and Cl4. The coordination polyhedron is strongly distorted toward a tetrahedron, the dihedral angles between best planes through Cl3–Cu1–Cl4 and N23–Cu1–N13 being equal to  $43.98(13)^\circ$ . The Cu2 is coordinated by the imidazolate nitrogen N21, the pyrazole nitrogens N32 and N42, the tertiary amine N17, and the chloride ion Cl5. The coordination environment formed by this donor atom set is best described by a distorted square-base pyramid, as the bond distances of the mutually opposite donor atoms are practically equal (Berry pseudorotation = 89%).

In compound **2** the Cu1 ion is coordinated by the imidazole nitrogen N13 and three chloride ions Cl2, Cl3, and Cl4. The coordination polyhedron is almost a tetrahedron. The Cu2 ion is coordinated by the imidazole nitrogen N21, the pyrazole nitrogens N32 and N42, the tertiary amine N17, and the chloride ion Cl5. The environment formed by this donor atom set is again described by a distorted square-base pyramid (Berry pseudorotation = 90%).

Although the best plane passing through the atoms N17, N21, Cl5, and N32 is nearly at the same distance from the donor atoms in both compounds **1** and **2**, the copper(II) ion labeled Cu2 is above the best plane passing through the donor atoms N17, N21, N32, and Cl5 of 0.176 and 0.292 Å, respectively. The apical bond Cu2–N42 is out of the perpendicular by 7.4 and  $2.2^\circ$  in **1** and **2**, respectively.

The complex **1** contains an imidazolate-bridging Cu1 and Cu2 and separating them by 5.566 Å. The two imidazolate nitrogens bind Cu2 at a distance of 1.919 Å and Cu1 at 1.942 Å. As there is no imidazolate bridge complex **2** accommodates the two copper(II) ions at a distance of 6.104 Å.

The bridging imidazolate ring of **1** is nearly planar with the largest deviation from the best plane being 0.007 Å. The imidazolate ring is distorted with C22–N21–C25, and C22–N23–C24 angles smaller than and N21–C22–N23 angle larger than  $108^\circ$ . This kind of distortion is typical for bridging-imidazolate ligands.<sup>10,34,35</sup> The other imidazole ring is perfectly planar and only slightly distorted. In compound **2**, the imidazole rings are planar with deviation to the best planes within 0.007 Å. The pyrazole rings are planar with deviations to the least-squares planes within 0.005 Å for both complexes.

Hydrogen bond networks are present in both structures. In complex **1**, Cl3 is hydrogen-bonded to N11 {Cl3...N11 = 3.462(4) Å} in an infinite chain running in the *a*-axis direction. In complex **2** chlorines Cl2 and Cl3 are hydrogen-bonded to N11 and N23, respectively {Cl2...N11 = 3.292(5) and Cl3...N23 = 3.123(5) Å} in an infinite two-dimensional network perpendicular to the *b* axis.

No stacking between the rings is observed; therefore, the crystal packing is determined by van der Waals contact and hydrogen bonding.

**Magnetic Properties.** The graphical representation of complex **1** magnetic susceptibility per gram atom of copper at various temperatures is reported in Figure 3 as  $\chi$  vs  $T$ . The susceptibility passes through a maximum at about 85 K and then falls to a minimum at about 20 K. This behavior is characteristic of antiferromagnetic coupled compounds containing small amounts of paramagnetic impurity. The value of  $\chi T$

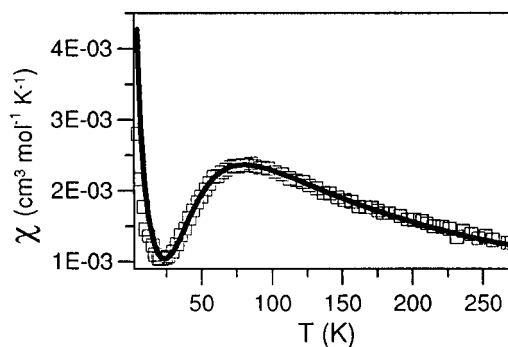


**Figure 3.** Magnetic susceptibility vs temperature plot for **1**. The solid line represents the calculated curve for the parameters  $-2J = 96 \text{ cm}^{-1}$ ,  $g = 2.025$ , and  $p = 0.05$ .

at 270 K is  $0.332 \text{ cm}^3 \text{ mol}^{-1}$  in agreement with the expected value for a coupled copper(II) ions. The susceptibility data were fitted by using the following equation:

$$\chi_{\text{calcd}} = p \frac{N\beta^2 g^2}{3kT} S(S+1) + (1-p) \frac{2N\beta^2 g^2}{kT} \frac{1}{3 + \exp(-2J/kT)}$$

Here,  $p$  is the paramagnetic impurity,  $-2J$  is the singlet-triplet separation and  $g$  the Landé factor. The first term represents the paramagnetic contribution and the second term is the Bleaney–Bowers equation for exchange-coupled pairs of copper(II) ions. The fitting was performed by minimizing the following function:

$$R^2 = \frac{\sum (\chi_{\text{obs}} - \chi_{\text{calcd}})^2}{\sum \chi_{\text{obs}}^2}$$

The fitting converged at  $-2J = 96 \text{ cm}^{-1}$  and  $g = 2.025$ , with  $p = 0.05$  and  $R^2 = 6.6 \cdot 10^{-5}$  ( $R = 0.0079$ ).

**EPR Studies.** For spin-coupled Cu(II) systems both  $\Delta M_s = \pm 1$  and  $\Delta M_s = \pm 2$  transitions are predicted.<sup>36</sup> For  $\Delta M_s = \pm 1$  transitions, theory predicts a group of peaks distributed around  $g \approx 2$  with line widths depending on the distance ( $r$ ) between the two copper(II) centers. At very short values of  $r$ , the EPR signal broadens and can be silent if the antiferromagnetic coupling is strong enough. In complex **1**, a value  $r$  of 5.566 Å was calculated from diffractometric studies. At this distance a broad spectrum is usually observed and very low temperatures are needed to detect a well-resolved signal.

The temperature dependence of the EPR spectrum of a powdered sample of complex **1** is shown in Figure 4. At the lowest temperatures, 9–14 K, peaks due to impurities of non-imidazolate-bridged copper(II) complexes dominate the EPR spectrum. In agreement with the magnetic susceptibility data obtained for this complex, the EPR signal becomes more intense as the temperature increases, although the spin–spin interaction causes a loss of resolution at higher temperature. The EPR spectrum of a powdered sample of the complex **1** at 77 K showed a fairly broad signal centered at  $g \approx 2.10$ . This solid-state broad peak agrees with the triplet signal detected in solution (vide infra). In contrast, the powder EPR spectrum of complex **2** showed two different features in the parallel region as this complex has the two copper centers not interacting with each other (lack of the imidazolate bridge). Unfortunately, these solid EPR spectra recorded on magnetically undiluted powdered samples are not informative.

On the contrary, the 77 K EPR spectrum of an aqueous frozen solution of **1** at pH 7.1 showed both the  $\Delta M_s = \pm 2$  (“half field” transition is observed at about 160 mT with a well-resolved

(34) Matsumoto, K.; Ooi, S.; Nakao, Y.; Mori, W.; Nakahara, A. *J. Chem. Soc., Dalton Trans.* **1981**, 2045.

(35) Haddad, M. S.; Duester, E. N.; Hendrickson, D. N. *Inorg. Chem.* **1979**, *18*, 141.

(36) Smith, T. D.; Pilbrow, J. R. *Coord. Chem. Rev.* **1974**, *13*, 173.

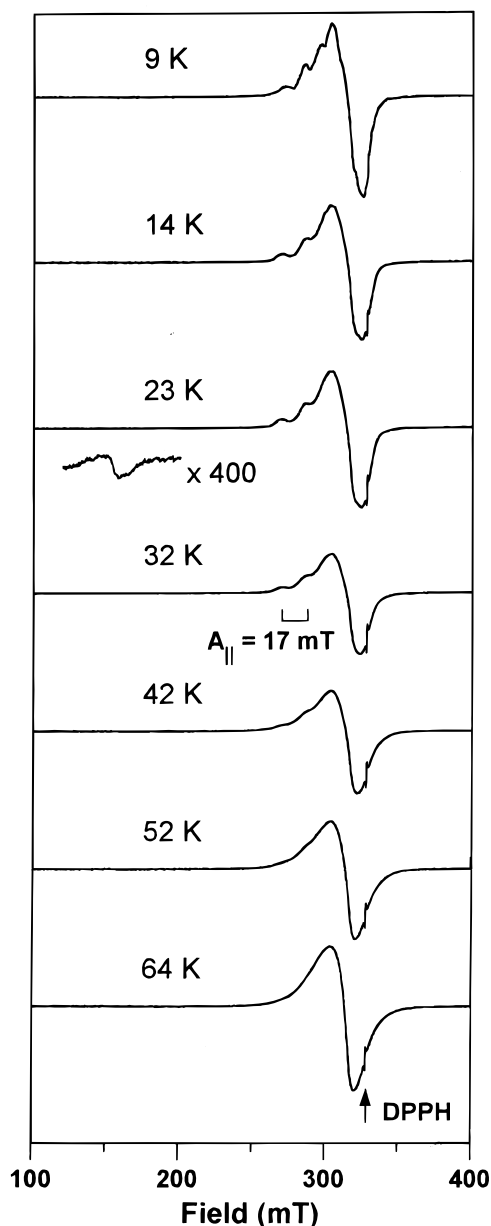


**Figure 4.** Temperature dependence of the EPR spectrum of solid **1**. Instrumental settings: microwave frequency, 9.088 GHz; modulation amplitude, 0.2 mT; time constant, 0.33 s; scan time, 420 s.

hyperfine structure), and the  $\Delta M_s = \pm 1$  region with a fairly broad signal at 318 mT and two flattened shoulders at 265 and 343 mT.

Decreasing the pH below 5.8 (see Figure 5) probably results in the disruption of the imidazolate bridge. Further pH decreasing leads to a complicate rearrangement of the ligand, involving the successive protonation of the different nitrogen donor atoms and the gradual release of “free” copper(II) ion, but even at pH 1.0 part of the copper(II) continues to be present as two separate species, the coordination environments of which are not easy to deduce. The spectrum of the frozen solution showed, in fact, the presence of the signal due to one or two species, in addition to those of the “free” copper(II) ion. If the pH above is allowed to rise 7.1, the dinuclear complex remains practically unchanged up to pH 8.2; above this pH value, the imidazolate bridge is broken again as seen from the appearance of a mononuclear pattern in the EPR spectrum. A probable competition by  $\text{OH}^-$  which can coordinate copper(II) substituting the imidazolate nitrogens must be taken into account. Finally at pH about 9.5 a brown precipitate started to separate.

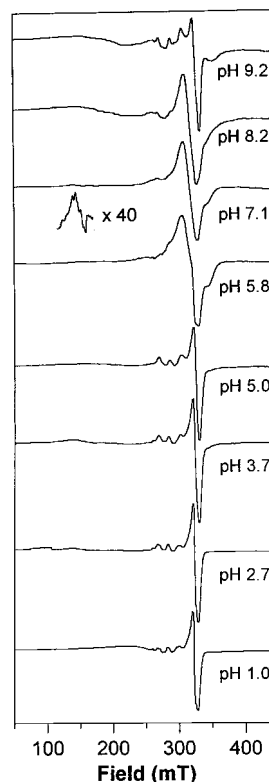


**Figure 5.** EPR spectrum of a 5 mM frozen aqueous solution of **1** as a function of pH. Instrumental settings: microwave frequency, 9.375 GHz; modulation amplitude, 0.7 mT; time constant, 0.33 s; scan time, 420 s.

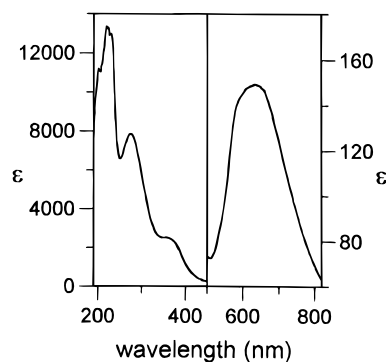


**Figure 6.** UV-vis spectrum of a 5 mM aqueous solution of **1** at pH 7.

So, the imidazolate-bridged complex **1** is stable from pH 5.8 to pH 8.2, hence covering the physiological pH range.

The 77 K EPR spectrum of powdered crystals of **2** showed two well-resolved signals in the parallel region, as a result of the different coordination of the two copper(II) ions. The 77 K frozen aqueous solution EPR spectrum of complex **2** exhibits the usual pattern for mononuclear copper(II) complexes and shows two signals due to the presence of two different copper(II) co-ordination environments, with parallel magnetic parameters of  $g_{\parallel} = 2.313 \pm 0.002$ ,  $A_{\parallel} = (149 \pm 3) \times 10^{-4} \text{ cm}^{-1}$  and  $g_{\parallel} = 2.255 \pm 0.002$ ,  $A_{\parallel} = (165 \pm 3) \times 10^{-4} \text{ cm}^{-1}$ , respectively.

**UV-Visible Spectroscopy.** The UV-visible spectrum of complex **1** at pH 7.0 is shown in Figure 6. This spectrum shows a fairly broad d-d band constituted by two peaks centered at 580 and 650 nm, respectively. In addition LMCT transitions are present and, in particular, the band at 375 nm is a sensitive parameter for the dicopper(II) imidazolate bridge formation.<sup>37</sup> This latter band is also present in the diffuse reflectance spectrum together with a broad d-d band composed of two

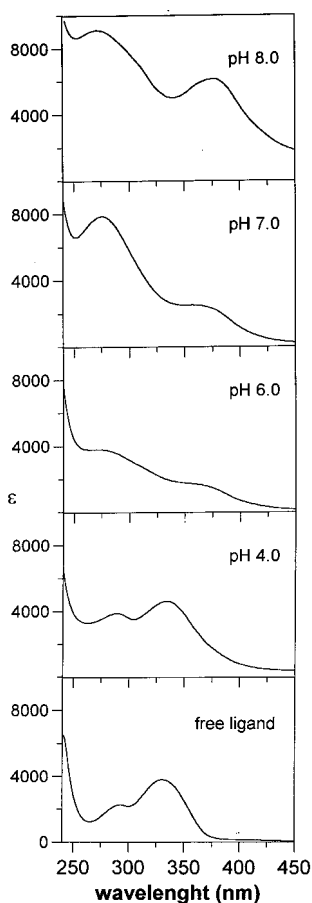


**Figure 7.** UV-vis spectrum of a 5 mM aqueous solution of **1** as a function of pH and free ligand for comparison.

absorptions centered at 616 and 725 nm, respectively. The formation of the imidazolate bridge was followed by monitoring the spectral changes in the LMCT region as a function of the pH, as shown in Figure 7. At pH 4.0 the spectrum displays a band at 334 nm which disappears when the pH is raised. A band at 375 nm progressively increased in intensity on going from pH 5 to pH 8. These results parallel that obtained from frozen solution EPR spectra: copper(II) is coordinated even for acidic pH values, but the imidazolate bridge formation begins at pH 5 and is completely formed between pH 7 and 8. The titration of the ligand itself in the same pH range showed a band centered at 334 nm, which remained unchanged over all pH values, and a band at 292 nm that only shifted to 286 nm at pH 4. The d-d transitions are shifted going from the solid to solution. This fact can be attributed to the different constraints imposed to the copper coordination sites by the packing in the solid state and to the coordination of water molecules that will replace the chlorides in aqueous solution.

**Cyclic Voltammetry.** The voltammetric behavior of complex **1** is characterized by one fairly broad peak both in the cathodic wave and in the anodic wave. The cathodic potential ( $E_{pc}$ ) shifted from  $-0.140$  to  $-0.268$  V/SCE, whereas the anodic potential ( $E_{pa}$ ) shifted from  $-0.034$  to  $0.078$  V, going to faster scan rates. The separation between potential peaks ( $\Delta E_p = E_{pa} - E_{pc}$ ) varies from 100 to 350 mV. This behavior is characteristic of quasi-reversible processes. On the basis of the width of the peaks it is probable that two redox steps are present, but only one broad peak is detected. Repetitive scans did not

show a different behavior; thus, a disproportionation process can be ruled out. The number of calculated electrons, hypothesizing either reversible or irreversible redox processes, was observed to be 1.7–2.0, thus suggesting that both copper ions participate to the overall reduction process with one electron each.

**SOD Activity.** The complex **1** exhibits significant catalytic activity toward the dismutation of superoxide anions. Superoxide was enzymatically supplied from the xanthine-xanthine oxidase system and the SOD activity was evaluated by the NBT assay,<sup>32</sup> following kinetically the reduction of NBT to  $MF^+$  at 560 nm. The concentration causing the 50% inhibition of NBT reduction (i.e.  $\Delta A_{560}/\text{min} = 0.012$ ) is called  $IC_{50}$ . The determined  $IC_{50}$  value has been found to be  $2.55 \times 10^{-7}$  M for complex **1**, which is higher than the value showed by native bovine erythrocyte SOD ( $4 \times 10^{-8}$  M), but on the same order of magnitude as the best SOD analogues described in the literature.<sup>6</sup> The monitored rate of uric acid formation was the same, in the presence and in absence of the copper(II) complex, ruling out any interference of complex **1** with the enzymatic system. It was also verified that, under the above-described experimental conditions, the eventual formation of copper phosphate species did not affect the result of the assay as demonstrated by Costanzo et al.<sup>22</sup>

## Discussion

The structures of the complexes **1** and **2** differ substantially by the presence or the absence, respectively, of an imidazolate bridge. The metal-nitrogen bond lengths are very similar for both metal sites in each complex. The imidazole nitrogen-copper(II) bond lengths are shorter than the copper-pyrazole bond lengths, i.e. 1.985, 1.942, and 1.919 Å in **1** and 2.039 and 1.938 Å in **2**. In particular, in complex **1**, the imidazolate nitrogen to copper(II) bond length is slightly shorter than the imidazole nitrogen to copper(II) length. This shorter distance can be ascribed to the increased basicity of the imidazolate moiety and is in agreement with the values described in the literature for other Cu(im)Cu complexes.<sup>6,8,38–40</sup>

Interestingly, in the case of complex **1**, the coordination geometry of the Cu1 is intermediate between square planar and tetrahedral as the planes Cu1–N13–N23 and Cu1–Cl3–Cl4 make an angle of  $43.9^\circ$ . In the case of complex **2** the atom Cu1 is practically tetrahedral, all coordination angles being near  $109.5^\circ$  within  $6.2^\circ$ . A strongly tetrahedral distorted geometry has been described for other copper(II) complexes containing the bis(imidazole) moiety<sup>41–44</sup> or sterically hindered azoles,<sup>45,46</sup> but it differs from other dicopper(II) complexes having similar ligands.<sup>47</sup>

In both complexes the atom Cu2 is found to be in a distorted square pyramid. This kind of geometry has been observed also

(37) Schugar, H. J. In *Copper Coordination Chemistry: Biochemical and Inorganic Perspectives*; Karlin, K. D., Zubietta J., Eds.; Adenine Press: New York, 1983.

- (38) Drew, M. G. B.; McCann, M.; Nelson, S. M. *J. Chem. Soc., Dalton Trans.* **1981**, 1868.  
 (39) Kolks, G.; Lippard, S. J. *Acta Crystallogr.* **1984**, C40, 261.  
 (40) Koolhaas, G. J. A. A.; Driessen, W. L.; van Koningsbruggen, P.; Reedijk, J.; Spek, A. L. *J. Chem. Soc., Dalton Trans.* **1993**, 3803.  
 (41) Knapp, S.; Keenan, T. P.; Zhang, X.; Fikar, R.; Potenza, J. A.; Schugar, H. J. *J. Am. Chem. Soc.* **1990**, 112, 3452.  
 (42) Ohkubo, S.; Inoue, K.; Tamaki, H.; Ohba, M.; Matsumoto, N.; Okawa, H.; Kida, S. *Bull. Chem. Soc. Jpn.* **1992**, 65, 1603.  
 (43) van Ooijen, J. A. C.; Reedijk, J.; Spek, A. L. *J. Chem. Soc., Dalton Trans.* **1979**, 1183.  
 (44) Valle, G.; Gonzalez A. S.; Ettore, R. *Acta Crystallogr.* **1991**, C47, 1392.  
 (45) Müller, E.; Bernardinelli, G.; Reedijk, J. *Inorg. Chem.* **1996**, 35, 1952.  
 (46) Bouwman, E.; Driessen, W. L.; Reedijk, J. *Coord. Chem. Rev.* **1990**, 104, 143.  
 (47) Koolhaas, G. J. A. A.; Driessen, W. L.; Reedijk, J.; Kooijman, H.; Spek, A. L. *J. Chem. Soc., Chem. Commun.* **1995**, 517.

for other di- or polycopper(II) complexes having bulky ligands.<sup>48,49</sup> In complex **1**, Cu2 is above the best plane passing through the basal donor atoms by 0.176 Å. In **2** this displacement is 0.292 Å. This difference may be due to the lack of an imidazolate bridge that, imposing less strain to the molecule, allows smaller C15–Cu2–N17 and N21–Cu2–N32 angles.

In the complex **1**, the N–C and C–C bonds of imidazolate range from 1.336 to 1.384 Å and the bond angles from 104.5 to 112.5°, values which are in agreement with those of other imidazolate-bridge complexes. The  $\alpha$  angles defined as Cu–N(im)–C2 angles in the imidazolate bridge of **1** range from 115.9° for Cu2–N21–C22, to 125.3° for Cu1–N23–C22, the former value being smaller than those generally observed. The value of 128.7° for the angle Cu1–N13–C12 is in good agreement with the values reported for bis(imidazole)copper(II) complexes.<sup>43,44</sup> From comparison with the angles Cu1–N13–C12 and Cu2–N21–C22 of **2**, which are 132.9 and 117.3°, respectively, coordination geometry constraints imposed by the ligand can be inferred.

The distances between the two copper(II) ions are 5.566(1) and 6.104(1) Å in **1** and **2**, respectively. These copper–copper distances are shorter than that found in SOD, in which the two metal centers are 6.3 Å apart. It is noteworthy that the ligand has a pocket-like site formed by the 1,5-bis(1-pyrazolyl)-3-[(2-imidazolyl)methyl]azapentane moiety that chelates copper(II).<sup>50–53</sup> The chelation of the first Cu probably favors the formation of the dinuclear species because it appears to orient the imidazole ring for the successive formation of the imidazolate bridge. This process seems so favored that even when the amount of added copper(II) salt is less than stoichiometric, complex **2** is formed. This hypothesis is strongly supported by the features of EPR spectra of the complex **1** in the pH range 1.0–5.0, in which patterns due to the progressive complexation of copper(II) in two different environments are present; at pH 5.8 a triplet signal as consequence of the deprotonation of the imidazole and formation of imidazolate bridge is evident.

The value of the magnetic exchange parameter  $-2J$  is indicative of the degree of interaction between the two unpaired electrons through the imidazolate-bridging and is related to the overlap of magnetic orbitals, depending, thus, on the structure of the complex. Several attempts of correlation between  $-2J$  and some structural parameters, such as the  $\alpha$ ,  $\beta$ , and  $\theta$  angles, have been undertaken in the literature.<sup>54–57</sup> In the complex **1** the  $\alpha_1$  angle of 125.3° for Cu1–N23–C22 is very close to those obtained for copper(II) complexes having similar values of  $-2J$ ,<sup>57</sup> but the similarity becomes less clear looking at the  $\alpha_2$  angle of 115.9° for Cu2–N21–C22. This smaller angle can be attributed to the coordination constraints imposed by the

ligand. Moreover, despite this latter angle, the  $|J|$  value is high indeed. Haddad et al.<sup>55</sup> examined the  $\alpha$  angles in a series of related compounds observing that an increase in  $\alpha$  angle, taking the imidazolate as reference point, should be correlated to an increase in magnetic exchange, i.e. in the absolute value of  $-2J$ . Any substituent on C2 should increase the  $\alpha$  angle, providing a stronger interaction between the two Cu(II) ions through the imidazolate bridge. Conversely, Kolks et al.<sup>56</sup> stated that no correlation exists, but only the imidazole  $pK_a$ 's could be related to  $-2J$ . This anomalous value reported for the dicopper complex **1** can be related with the basicity of the imidazolate moiety, supporting the hypothesis of Kolks.<sup>56</sup> In fact, although  $pK_a$ 's of this ligand were not determined, it is reasonable to assume that the electronic effect of the substituent in C2 would increase the basicity of the imidazolate itself.<sup>58</sup> Considering the  $\beta$  angle as well as the short bond distance Cu–N<sub>im</sub>, defined by Cu–N<sub>im</sub>–N<sub>im</sub>,<sup>25</sup> a very short bond distance is expected to produce a very large overlap between the metal and ligand orbitals. The relation between the bond length and the orbital overlap is very difficult to estimate, so as it is reasonable to assume a dependence of orbital overlap on  $1/r^2$ . The  $\beta$  angle shows a variability, ranging generally from 157 to 166°. When it approaches 180°, the magnetic exchange should be enhanced as in the chelating species [Cu<sub>2</sub>bpim]<sup>3+</sup>.<sup>59</sup> For complex **1**,  $\beta$  angles have been estimated as 153.5 and 146.3°, for Cu1 and Cu2, respectively. Although there is a strong similarity between **1** and the structurally related compounds cited above, in both  $\beta$  angles and  $-2J$ , it is not possible to establish a simple correlation between the structural parameters and the magnitude of the magnetic exchange. Most likely, several parameters affect the magnetic exchange and contribute to the overall interaction. The magnetic exchange is also affected by the angle  $\theta$ , the dihedral angle between the copper coordination plane and the imidazolate ring. The value of  $-2J$  in **1**,  $-96 \text{ cm}^{-1}$ , is larger than the values found for many other imidazole-bridged complexes,<sup>34,57,60</sup> and on the same order of magnitude as those of some related complexes, [Cu<sub>6</sub>(tidah)<sub>2</sub>Cl<sub>10</sub>(H<sub>2</sub>O)<sub>4</sub>] and [Cu<sub>2</sub>(bidph)(NO<sub>3</sub>)<sub>2</sub>(H<sub>2</sub>O)<sub>2</sub>].<sup>40,61</sup> The values of  $\theta$  are 41.0 and 20.6°, considering the coordination environment least-square planes for Cu1 and Cu2, respectively. This discrepancy becomes smaller if the angles between the Cu–N<sub>im</sub> vectors and the imidazolate ring are considered. They reduce to 19.0 and 17.8°, for Cu1 and Cu2, respectively.

It is of substantial interest that the magnetic behavior of complex **1** is present also in aqueous solution, as the imidazolate bridge is retained as demonstrated by both pH-dependent frozen solution EPR spectra and pH-dependent UV–vis spectra. On the other hand, we are interested in this kind of behavior, in order to study a possible use of this dinuclear complex as catalyst against superoxide radical. The SOD-like activity of complex **1** is one of the highest in the literature, and notably, at physiological pH, the dinuclear complex is stable, so it can be considered a good model for SOD.

In the experimental conditions used to evaluate the SOD-like activity the phosphate ion is present in a very large excess with respect to complex **1**, and the ratio of [HPO<sub>4</sub><sup>2-</sup>] to [Cu]<sub>tot</sub> is about 40 000. It has been demonstrated that the species [Cu(HPO<sub>4</sub>)] is much less active than some dipeptide copper(II) complexes and obviously less than the native enzyme itself.<sup>22</sup> Thus, the extremely high activity of complex **1** could not be

- (48) van Albada, G. A.; Haasnoot, J. G.; Reedijk, J.; Biagini-Cingi, M.; Manotti-Lanfredi, A. M.; Ugozzoli, F. *Polyhedron* **1995**, *14*, 2467.  
 (49) Bol, J. E.; Driessen, W. L.; Reedijk, J. *J. Chem. Soc., Chem. Commun.* **1995**, 1365.  
 (50) Tran, K. C.; Battioni, J. P.; Zimmerman, J. L.; Bois, C.; Koolhaas, G. J. A. A.; Leduc, P.; Mulliez, E.; Boumchita, H.; Reedijk, J.; Chottard, J. C. *Inorg. Chem.* **1994**, *33*, 2808.  
 (51) van Berkel, P. M.; Driessen, W. L.; Koolhaas, G. J. A. A.; Reedijk, J.; Sherrington, D. C. *J. Chem. Soc., Chem. Commun.* **1995**, 147.  
 (52) Haanstra, W. G.; Cabral, M. F.; de O. Cabral, J.; Driessen, W. L.; Reedijk, J. *Inorg. Chem.*, **1992**, *31*, 3150.  
 (53) Driessen, W. L.; Haanstra, W. G.; Reedijk, J. *Acta Crystallogr.* **1992**, *C48*, 1585.  
 (54) Bencini, A.; Benelli, C.; Gatteschi, D.; Zanchini C. *Inorg. Chem.* **1986**, *25*, 398.  
 (55) Haddad, M. S.; Hendrickson, D. N. *Inorg. Chem.* **1978**, *17*, 2622.  
 (56) Kolks, G.; Lippard, S. J.; Waszczak J. V.; Lilienthal, H. R. *J. Am. Chem. Soc.* **1982**, *104*, 717.  
 (57) Chaudhuri, P.; Karpstein, I.; Winter, M.; Lengen, M.; Butzlaff, C.; Bill, E.; Trautwein, A. X.; Flörke, U.; Haupt, H.-J. *Inorg. Chem.* **1993**, *32*, 888.

- (58) Hay, P. J.; Thibeault, J. C.; Hoffman, R. *J. Am. Chem. Soc.* **1975**, *97*, 4884.  
 (59) Dewan, J. C.; Lippard, S. J. *Inorg. Chem.* **1980**, *19*, 2079.  
 (60) Mao, Z. W.; Chen, D.; Tang, W. X.; Yu, K. B.; Liu, L. *Polyhedron* **1992**, *11*, 191.  
 (61) Koolhaas, G. J. A. A. Ph.D. Thesis, Leiden, The Netherlands 1996

due to the formation of some amount of  $[\text{Cu}(\text{HPO}_4)]$  species. Moreover, in the presence of this latter species, the active concentration ( $\text{IC}_{50}$ ) of complex **1** is lower than the apparent one. In other words, this complex is actually more active than apparently observed, so as the catalytic activity should be nearer to the SOD one.

The SOD activity is related to the equatorial field experienced by the copper(II) ion.<sup>18–23</sup> A strong equatorial field opposes the interaction of the complexed copper with superoxide radical, unfavoring the probable formation of the intermediate copper–superoxide adduct.<sup>18</sup> Moreover, a strong field is a factor which disfavors the reduction process from copper(II) to copper(I). Another important factor in the catalytic process is the ability of the ligand to accommodate the reduced copper(I) in a tetrahedral-like or linear environment.<sup>62</sup> Therefore, designing ligands having a flexible backbone capable to accommodate the copper ion in different geometries or alternatively ligands having a limited flexibility but imposing a tetrahedral-like constrains, is an important goal. The ligands Hbpzbiap and bpzbiap—fall in this latter case. The tetrahedral distortion imposed by these ligands to copper(II) ion in both complexes is of particular importance because it can allow a more easy reduction of copper(II) ion.<sup>63</sup>

The reduction process of complex **1** was quasi-reversible and two electrons are involved. The reduction of the two copper(II) seems to happen in a very narrow range. In fact, the peaks detected are fairly broad and no more peaks were found. The increased  $\Delta E_p$  is a sensible indicator of the reversibility of the electrochemical process. Nevertheless, we normally assume that in the electrochemical process the species that undergo the re-oxidation retain the same environment, i.e. that bond lengths and angles remain alike or equal. In contrast, it can occur that the reduced copper(I) is not really tetrahedral or tetrahedral-like, and some donor atom distances may temporarily stretched out. Consequently, the coordination environment could become linear, and the re-oxidation process takes place at different potential values. Unless disproportionation processes occur, the re-oxidized species can reconstitute the original coordination environment. Therefore,  $\Delta E_p$  is an absolute parameter for the electrochemical reversibility, but the catalytic cycle is assured even in presence of quasi-reversible electron transfer processes. The reduction potential of complex **1** is lower than 0.115 and 0.075 V/SCE, values obtained at pH 7.4 for the bovine and human SOD enzyme, respectively,<sup>64</sup> but in a very good range

for promoting the dismutation of superoxide anion as showed by the high catalytic activity.

Some authors have emphasised that the way of generation of superoxide anion is important. In fact, the concentration of superoxide anions supplied by radiolysis techniques is high enough to provide a levelling effect for many copper(II) complexes that appear to possess a scavenger activity very similar to SOD.<sup>6,65</sup> Using a biological source, such as the system xanthine–xanthine oxidase, the amount of superoxide supplied is much lower (about  $10^{-11}$  M) and stationary. This method provides a way to differentiate among the scavenging ability of copper(II) complexes.

### Concluding Remarks

The results described in the present paper have clearly demonstrated that careful design of a new ligand can indeed lead to a novel, asymmetric dinucleating system, which does bind Cu strongly. The backbone of the ligands Hbpzbiap and bpzbiap<sup>−</sup> allows to accommodate the copper ion in both Cu(I) and Cu(II) states because of their degree of flexibility and some constrains imposed by the ligands themselves. The imidazolato-bridge complex is stable in a pretty wide pH range, which includes pHs around the physiological values, and it has shown a significant SOD activity. Voltammetric studies gave evidence to a quasi-reversible process that could be attributed to a dynamic rearrangement of the coordination environment during the redox process. Although the reduction potential of complex **1** is lower than that of the native protein, a very good catalytic activity is present.

The next phase in this study will deal with the binding of other metals and with heterodinuclear compounds. These investigations are in progress.

**Acknowledgment.** The Leiden authors are indebted to the EU for a grant as Host Institute in the EU Programme Human Capital and Mobility (1994–1997). The collaboration between the Leiden and Catania groups was supported by a Network from the European Union, Contract No. ERBCHRXCT920014, allowing regular exchange of preliminary results with several European colleagues. Also support coordinated by COST Action D1/0005/95 (Biocoordination Chemistry) is kindly acknowledged. This work was supported in part by the Netherlands Foundation of Chemical Research (SON) with financial aid from the Netherlands Organization for Scientific Research (NWO).

**Supporting Information Available:** Tables of fractional atomic coordinates, anisotropic thermal parameters, and interatomic bond lengths and angles, a plot of  $\chi T$  vs  $T$ , the EPR spectrum of a 5 mM frozen solution of **1** at pH 7.1, and the powder and frozen solution EPR spectra of **2** (11 pages). Ordering information is given on any current masthead page.

IC961260D

(62) Bonomo, R. P.; Conte, E.; Impellizzeri, G.; Pappalardo, G.; Purrello, R.; Rizzarelli, E. *J. Chem. Soc. Dalton Trans.*, **1996**, in press.

(63) Nishida, Y.; Unoura, K.; Watanabe, I.; Yokomizo, T.; Kato, Y. *Inorg. Chim. Acta*, **1991**, *181*, 141.

(64) (a) Azab, H. A.; Banci, L.; Borsari, M.; Luchinat, C.; Sola, M.; Viezzoli, M. S. *Inorg. Chem.* **1992**, *31*, 4649. (b) Ellerby, L. M.; Cabelli, D. E.; Graden, J. A.; Valentine, J. S. *J. Am. Chem. Soc.* **1996**, *118*, 6556–6561. (c) Lu, Y.; Roe, J. A.; Bender, C. J.; Peisach, J.; Banci, L.; Bertini, I.; Gralla, E. B.; Valentine, J. S. *Inorg. Chem.* **1996**, *35*, 1692–1700.

(65) Czapski, G.; Goldstein, S. *Free Radical Res. Commun.* **1988**, *4*, 225.